Formation of Intrathermocline Lenses by Eddy–Wind Interaction

DENNIS J. MCGILLICUDDY, JR.

Woods Hole Oceanographic Institution, Woods Hole, Massachusetts

(Manuscript received 28 October 2014, in final form 16 December 2014)

ABSTRACT

Mesoscale intrathermocline lenses are observed throughout the World Ocean and are commonly attributed to water mass anomalies advected from a distant origin. An alternative mechanism of local generation is offered herein, in which eddy–wind interaction can create lens-shaped disturbances in the thermocline. Numerical simulations illustrate how eddy–wind-driven upwelling in anticyclones can yield a convex lens reminiscent of a mode water eddy, whereas eddy–wind-driven downwelling in cyclones produces a concave lens that thins the mode water layer (a cyclonic ''thinny''). Such transformations should be observable with long-term time series in the interiors of mesoscale eddies.

1. Introduction

The midocean is populated by a variety of different types of eddies. Most common are cyclones and anticyclones with vertical structures characteristic of the first baroclinic mode (Gill et al. 1974; McWilliams and Flierl 1976; Wunsch 1997), which tend to raise and lower the main thermocline, respectively (Fig. 1, left column). However, more complex vertical structures are not uncommon. Specifically, so-called mode water eddies consist of a bolus of fluid that depresses the main thermocline and raises the seasonal thermocline (Fig. 1, upper right). Displacement of the main thermocline dominates both geostrophic velocity and sea level perturbations, such that these anticyclonic features are clearly detectable as positive sea level anomalies in satellite altimetry. The analogous second baroclinic mode structure in the cyclonic case is upward displacement of the main thermocline and downward displacement of the seasonal thermocline, resulting in a thinning of the mode water layer—thus, the term ''cyclonic thinny'' (Fig. 1, lower right). Again the main thermocline signal dominates, and such cyclones are readily detectable as negative anomalies in sea level.

Two such eddies were the subject of detailed in situ process studies in the Sargasso Sea, mode water eddy A4 and cyclonic thinny C1 (McGillicuddy et al. 2007). Both features had origins that could be traced back considerable distances from where they were sampled, as revealed by water mass analysis, transient tracer distributions, and backtracking of their trajectories via satellite altimetry (Jenkins et al. 2008; Li et al. 2008; McGillicuddy et al. 2007). As such, their complex vertical structure is attributable at least in part to their nonlocal origins. In the case of A4, a bolus of mode water formed south of the Gulf Stream could have been subducted, subsequently penetrating into the Sargasso Sea as a mesoscale eddy (e.g., Ebbesmeyer and Lindstrom 1986). In the case of C1, there was a clear signature of subtropical underwater (Schmitz and Richardson 1991) at the eddy center in a thin stratum where mode water was nearly absent; its water mass and biogeochemical characteristics suggest it may have been advected from the southern Sargasso Sea (Li et al. 2008).

Despite the nonlocal contributions to the vertical structure of these two eddies, it is of interest to discern whether or not the general sense of the isopycnal displacements could also be explained by local forcing of the eddies themselves. Specifically, inclusion of the surface current in the calculation of the wind stress can yield mesoscale variations in Ekman divergence. That is, higher stress occurs on the flank of the eddy where the wind opposes the surface current, with lower stress on the flank of the eddy where the wind and the current are in the same direction. The net result is Ekman suction (upwelling) in the interiors of anticyclones (Dewar and Flierl 1987; Martin and Richards 2001) and Ekman

Corresponding author address: Dennis J. McGillicuddy, Jr., Department of Applied Ocean Physics and Engineering, Woods Hole Oceanographic Institution, 98 Water St., Woods Hole, MA 02543.
E-mail: dmcgillicuddy@whoi.edu

DOI: 10.1175/JPO-D-14-0221.1

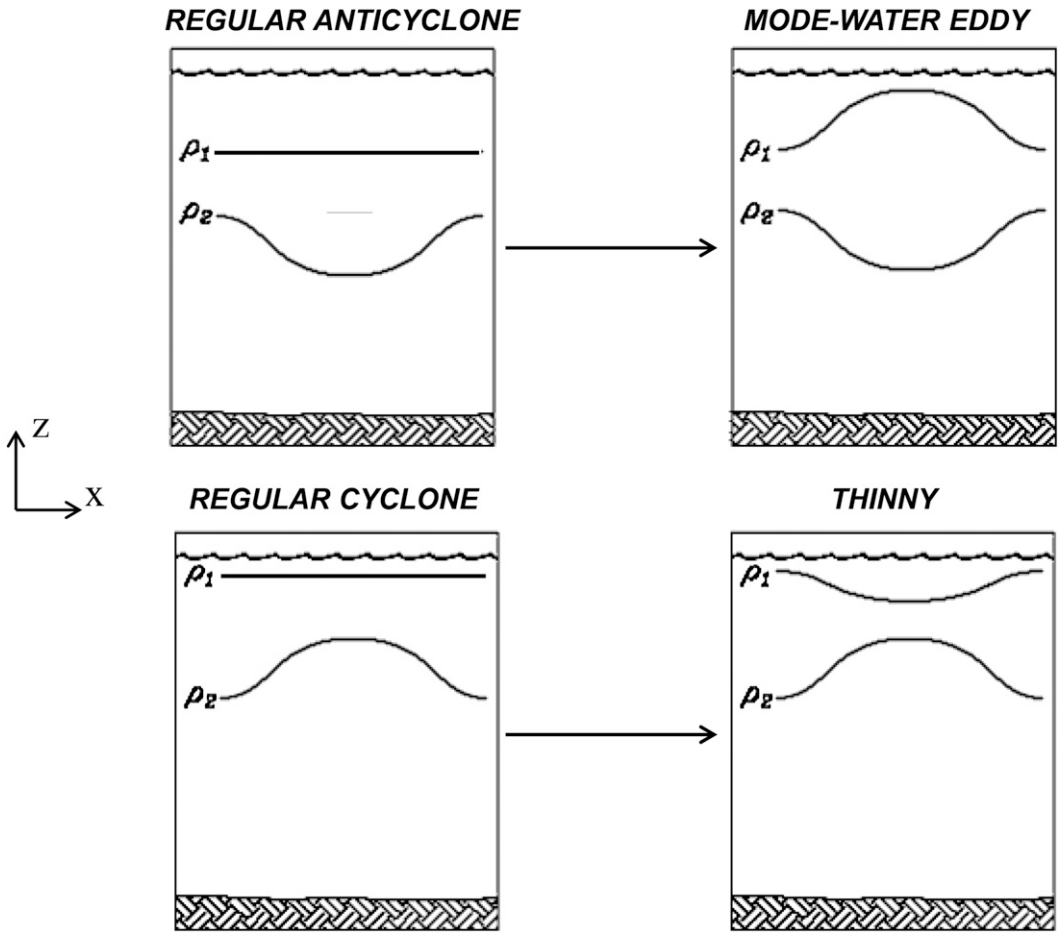

FIG. 1. Hypothesized transformations of a (top) regular anticyclone into a mode water eddy and (bottom) a regular cyclone into a cyclonic thinny. Each cross section depicts an isopycnal in the seasonal ρ_1 and main thermocline ρ_2.

pumping (downwelling) in the interiors of cyclones (Gaube et al. 2015b). This effect would tend to dome the seasonal thermocline in anticyclones and depress it in cyclones, thus potentially transforming these features into intrathermocline lenses (Fig. 1). This idea is tested by comparing the results of idealized models of isolated eddies forced by a standard wind stress formulation to those that include eddy–wind interaction.

2. Methods

The Parallel Ocean Program (POP; Smith et al. 1992; Smith et al. 2000) was used for the numerical experiments. This primitive equation model uses level coordinates and includes a free surface. The configuration is the same as described in Ledwell et al. (2008). Specifically, simulations are run in a 500 km^2 doubly periodic domain with 2.88-km horizontal resolution. The vertical grid has 72 levels, with resolution decreasing gradually from 5 m at the surface to 125 m at depth and with the bottom located at 4462 m. Subgrid-scale horizontal mixing is parameterized with a Laplacian operator of 1 $m^2 s^{-1}$. Vertical mixing is specified by the *K*-profile method (Large et al. 1994) with a background diffusivity of 10^{-5} $m^2 s^{-1}$ (Ledwell et al. 1993, 1998). To simplify diagnostics of the results in eddy-centric coordinates, the model is configured on an *f* plane to prevent the eddies from propagating.

Initial conditions (Fig. 2) consist of an isolated eddy at the center of the model domain. Radially symmetric temperature T and salinity S distributions are specified from average profiles inside and outside the eddy of interest:

$$T(r,z) = T_{\text{out}}(z) + [T_{\text{in}}(z) - T_{\text{out}}(z)] \exp\left(-\frac{r^2}{r_0^2}\right),$$

$$S(r,z) = S_{\text{out}}(z) + [S_{\text{in}}(z) - S_{\text{out}}(z)] \exp\left(-\frac{r^2}{r_0^2}\right),$$

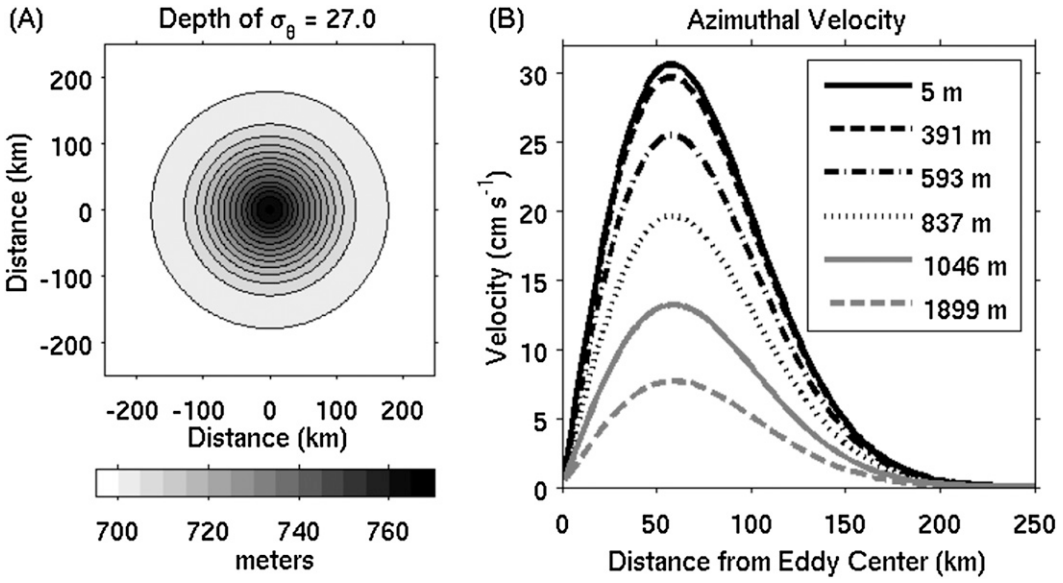

FIG. 2. Initial conditions for an idealized anticyclone with a downward displacement of the main thermocline similar to that of mode water eddy A4. (a) Depth of the σ_θ = 27.0 isopycnal and (b) azimuthal velocity. Corresponding initial conditions for cyclone C1 are not shown. See Figs. 3a and 4a for vertical sections of density in the initial conditions for A4 and C1, respectively.

where r_0 is the eddy radius inferred from hydrographic data. Temperature and salinity surfaces are assumed to be flat in the upper ocean ($z < 150$ m). This constitutes a departure from the typical first baroclinic mode structure, but it facilitates clearer analysis of the disturbance of near-surface isopycnals by eddy–wind interaction.

To prescribe velocities that are in approximate balance with the density field, initial velocity fields are computed as the sum of geostrophic and cyclostrophic contributions, assuming no motion at the bottom. The cyclostrophic terms constitute small corrections to the geostrophic velocities. Modest adjustment of the interior velocity fields in the first few days of the simulation attests to the efficacy of the initialization procedure.

Two runs were conducted for each eddy (Table 1): one with the standard wind stress τ formulation

$$\tau = \rho_{\text{air}} c_d u_{\text{air}} |u_{\text{air}}|$$

and one in which the stress is computed as the difference between air and ocean surface velocities u_{air} and u_{sea},

$$\tau = \rho_{\text{air}} c_d (u_{\text{air}} - u_{\text{sea}}) |u_{\text{air}} - u_{\text{sea}}|,$$

where ρ_{air} is the density of air, and c_d is the drag coefficient, which is specified according to Large and Pond (1981). The spatially uniform wind has a speed of 6.7 m s^{-1}, which is characteristic of summertime conditions in the region of the Sargasso Sea where eddies A4 and C1 were observed. To preserve the radial and azimuthal symmetry of the simulated eddies, the wind direction is assumed to rotate clockwise through a complete circle every 64 h. The specified period of wind rotation is somewhat arbitrary, although the key to maintaining symmetry is a period short enough to prevent significant net Ekman transport in the horizontal direction. A second consideration is avoiding resonance with the local inertial frequency (circa 24 h). This ad hoc rotation of the wind vector successfully maintains eddy-centric symmetry in the simulations, thereby simplifying the analysis.

In the absence of surface heating, wind forcing will cause deepening of the mixed layer. To balance the input of turbulent kinetic energy by the wind, surface heat fluxes are applied. A shortwave heat flux of 241 W m^{-2} into the ocean is specified (mean of shipboard measurements, assuming a 4% albedo). Sensible, latent, and long-wave heat fluxes are computed via bulk formulae. The resulting net heat flux is positive, thus maintaining a mixed layer depth that is roughly consistent with the observations.

TABLE 1. Summary of numerical simulations.

Run	Eddy	Wind stress
1	A4	$\tau = \rho_{\text{air}} c_d u_{\text{air}} \lvert u_{\text{air}} \rvert$
2	A4	$\tau = \rho_{\text{air}} c_d (u_{\text{air}} - u_{\text{sea}}) \lvert u_{\text{air}} - u_{\text{sea}} \rvert$
3	C1	$\tau = \rho_{\text{air}} c_d u_{\text{air}} \lvert u_{\text{air}} \rvert$
4	C1	$\tau = \rho_{\text{air}} c_d (u_{\text{air}} - u_{\text{sea}}) \lvert u_{\text{air}} - u_{\text{sea}} \rvert$

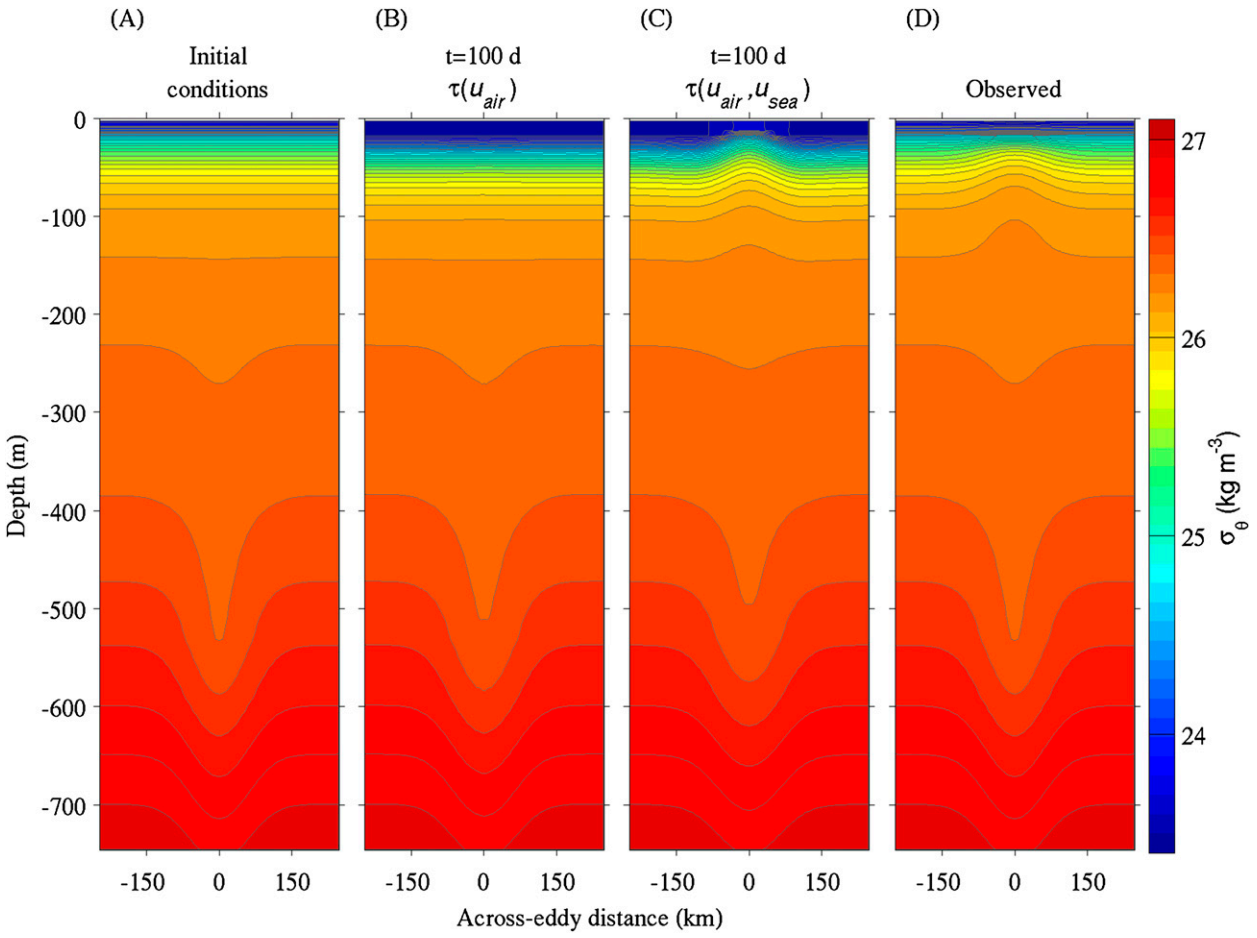

FIG. 3. Simulated and observed cross sections. (a) Initial condition for an anticyclonic eddy with a main thermocline displacement similar to mode water eddy A4 and flat near-surface isopycnals. Results after 100 days of integration (b) without and (c) with eddy–wind interaction, respectively. (d) Observed cross section of mode water eddy A4.

3. Results

After 100 days of integration in the anticyclonic case with the uniform wind stress formulation, near-surface isopycnals remain flat as in the initial condition (Figs. 3a,b). The mixed layer deepens due to the turbulence created by the wind stress, partially arrested by the decrease in surface density due to the heat flux. In contrast, the run with eddy–wind interaction exhibits upward doming of the near-surface isopycnals (Fig. 3c) as a result of upwelling at eddy center and flow into the eddy interior at intermediate depths. At day 100, the magnitude of the isopycnal displacements is comparable to those observed in eddy A4 (Fig. 3d). Note that the simulation with eddy–wind interaction shows some shoaling of the depressed isopycnals in the main thermocline (500–700 m) relative to the run without eddy–wind interaction, consistent with findings that this mechanism accelerates eddy decay (Dewar and Flierl 1987; Eden and Dietze 2009; Zhai and Greatbatch 2007).

Similarly, in the cyclonic case, near-surface isopycnals remain flat in the simulation with uniform wind stress (Figs. 4a,b). When the eddy–wind interaction effect is included, near-surface isopycnals are deflected downward by convergence at the eddy center, with flow out of the eddy at intermediate depths causing thinning of the mode water layer in the seasonal thermocline (Fig. 4c). This isopycnal topography is qualitatively similar to that observed, although the data contain small-scale structure that is not represented in the model. As in the anticyclonic case, eddy–wind interaction accelerates eddy decay, as evidenced by a reduction in the doming of main thermocline isopycnals.

In both the cyclonic and anticyclonic cases, the deflection of isopycnals associated with eddy–wind interaction is relatively monotonic in time (not shown). This stems primarily from the fact that the magnitude of

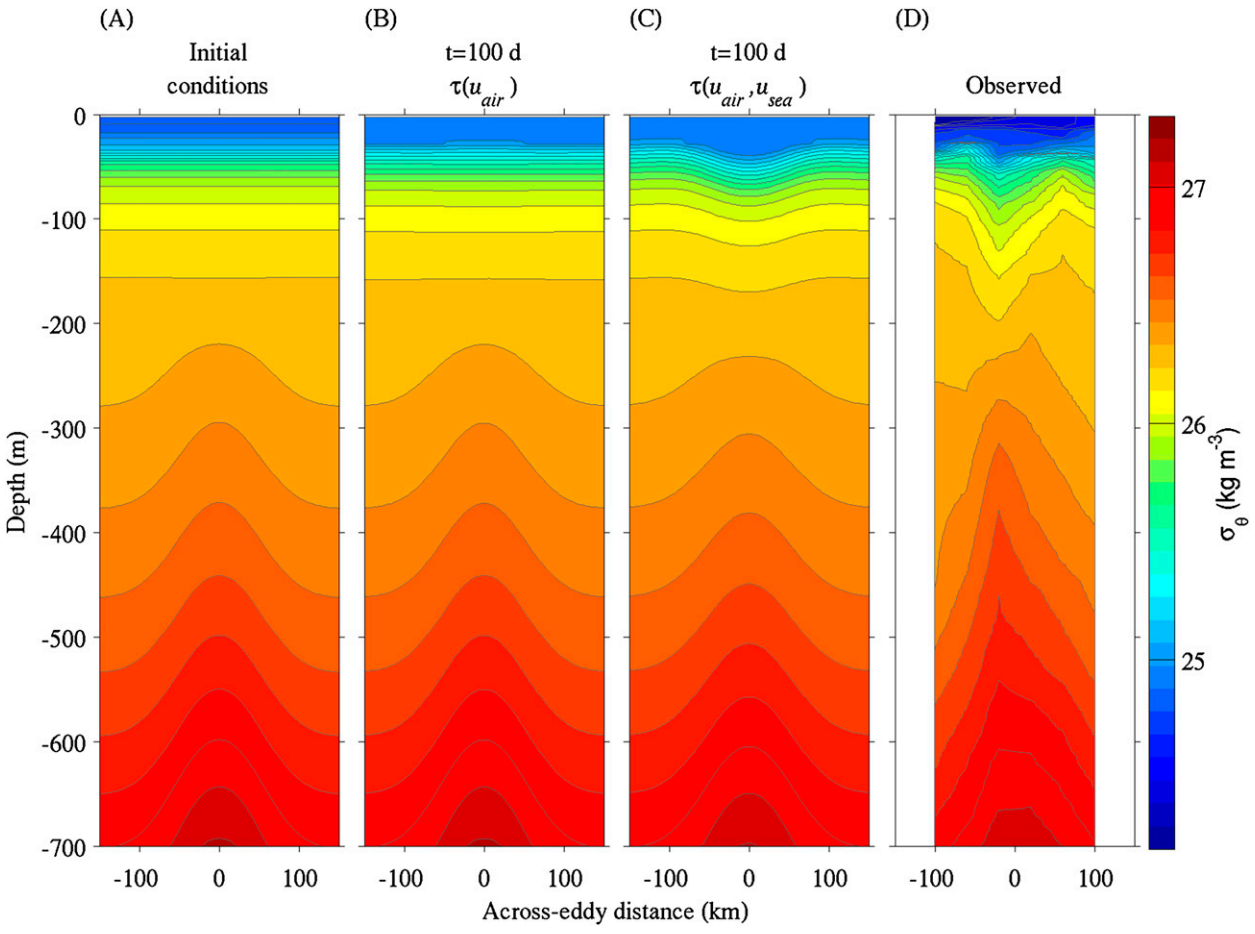

FIG. 4. Simulated and observed cross sections. (a) Initial condition for a cyclonic eddy with a main thermocline displacement similar to cyclonic thinny C1 and flat near-surface isopycnals. Results after 100 days of integration (b) without and (c) with eddy–wind interaction, respectively. (d) Observed cross section of cyclonic thinny C1.

the wind forcing is constant. However, because the eddies decay over time, there is a slight decrease in the magnitude of the eddy–wind-induced vertical velocity (more details below), resulting in a slowing of isopycnal displacements during the simulation.

Inclusion of the surface currents in the wind stress formulation can also bring about spatial variations in mixing. Specifically, the input of turbulent kinetic energy is higher where the wind and the surface current oppose each other and lower where the wind and surface current are in the same direction. However, the wind is constantly rotating in these simulations, thereby tending to smooth out such variations in the azimuthal direction. A more pronounced (but still modest) effect on mixed layer depth results from eddy–wind-induced isopycnal displacements, with shallower (deeper) mixed layer depths inside the anticyclone (cyclone) where upwelling (downwelling) increases (decreases) stratification (Figs. 3c, 4c).

4. Discussion

The model results demonstrate that eddy–wind interactions can create intrathermocline lenses with isopycnal topographies that are qualitatively similar to observations. However, it is important to note that congruence between the simulations and observations (Figs. 3, 4) reflects only a snapshot in time—if the simulations were run out over a longer period, one could expect continued increases in the amplitude of the upper-ocean isopycnal displacements and decay of the main thermocline perturbations. Of course, the time period of the simulations is rather arbitrary, especially in light of the idealized nature of the initial conditions in the upper ocean. It may be that at the time of eddy formation, upper-ocean isopycnal displacements could have the same sense as those of the main thermocline (upward in cyclones and downward in anticyclones). In that case, it would take longer for the eddy transformations (standard

anticyclone to mode water eddy and standard cyclone to cyclonic thinny) to take place.

The simulated displacements of upper-ocean isopycnals are consistent with vertical velocities w_E predicted by the scale analysis of Gaube et al. (2015a):

$$w_E = -\frac{3\rho_{\text{air}} c_d |u_{\text{air}}|}{2\rho_0 f}\zeta_{z=0},$$

where $\zeta_{z=0}$ is the relative vorticity of the eddy at the surface, and ρ_0 is the density of water. With relative vorticities of circa $0.1f$, the expected vertical velocities at the base of the Ekman layers in A4 and C1 are on the order of $0.1\,\text{m day}^{-1}$ for the specified wind conditions. This is sufficient to explain the rate at which upper-ocean isopycnals are displaced in the simulations. As described in Dewar and Flierl (1987), the magnitude of the vertical motion decreases with depth from the base of the Ekman layer into the main thermocline, and thus the deeper isopycnals are disturbed less than those above.

In both cyclonic and anticyclonic cases, the deflection of upper-ocean isopycnals creates geostrophic shear that is opposite in sign to that associated with the eddy-driven displacement of the main thermocline. This reduces the relative vorticity at the surface, thus decreasing the amplitude of the eddy–wind-induced Ekman pumping w_E. This will continue until the relative vorticity at the surface goes to zero, presumably leaving an intrathermocline lens intact, in which the upper ocean and main thermocline geostrophic shears exactly compensate each other at the surface.

5. Conclusions

This mechanism of local generation of intrathermocline lenses constitutes a hypothesis in need of testing with observations. Long-term time series within eddies are required to do so, and acquisition of such observations via shipboard surveys may prove to be impractical. Satellite data may be useful for this purpose, particularly given the utility of altimetry in eddy tracking (Chelton et al. 2011) and the capability to observe eddy–wind interaction in scatterometer measurements (Gaube et al. 2015a). Unfortunately, on the basis of sea level alone, it is not possible to differentiate regular anticyclones from mode water eddies nor regular cyclones from cyclonic thinnies. Autonomous floats and gliders offer an attractive approach to monitoring long-term changes in the isopycnal topography within eddies, particularly if they could be strategically deployed in newly formed eddy features identified in satellite data. These observations could be synthesized in the context of additional numerical experiments, especially in more realistic settings than the idealized simulations described herein. Such a combination of models and observations would be ideally suited to investigating the formation of intrathermocline lenses in the ocean, particularly in light of the intermittency of the underlying processes.

Acknowledgments. Support of this research by the National Science Foundation and National Aeronautics and Space Administration is gratefully acknowledged. I thank Bill Dewar for feedback during the initial analysis of the results and Peter Gaube and John Marshall for comments that helped improve the manuscript. Larry Anderson carried out the model runs and provided technical assistance in figure preparation. The simulations were conducted on high-performance computers (ark:/85065/d7wd3xhc) provided by NCAR's Computational and Information Systems Laboratory, sponsored by the National Science Foundation.

REFERENCES

Chelton, D. B., M. G. Schlax, and R. M. Samelson, 2011: Global observations of nonlinear mesoscale eddies. *Prog. Oceanogr.,* **91,** 167–216, doi:10.1016/j.pocean.2011.01.002.

Dewar, W. K., and G. R. Flierl, 1987: Some effects of wind on rings. *J. Phys. Oceanogr.,* **17,** 1653–1667, doi:10.1175/1520-0485(1987)017<1653:SEOTWO>2.0.CO;2.

Ebbesmeyer, C. C., and E. J. Lindstrom, 1986: Structure and origin of 18C water observed during the POLYMODE local dynamics experiment. *J. Phys. Oceanogr.,* **16,** 443–453, doi:10.1175/1520-0485(1986)016<0443:SAOOWO>2.0.CO;2.

Eden, C., and H. Dietze, 2009: Effects of mesoscale eddy/wind interactions on biological new production and eddy kinetic energy. *J. Geophys. Res.,* **114,** C05023, doi:10.1029/2008JC005129.

Gaube, P., D. B. Chelton, R. M. Samelson, M. G. Schlax, and L. W. O'Neill, 2015a: Satellite observations of mesoscale eddy-induced Ekman pumping. *J. Phys. Oceanogr.,* **45,** 104–132, doi:10.1175/JPO-D-14-0032.1.

——, D. J. McGillicuddy, D. B. Chelton, M. J. Behrenfeld, and P. G. Strutton, 2015b: Regional variations in the influence of mesoscale eddies on near-surface chlorophyll. *J. Geophys. Res. Oceans,* doi:10.1002/2014JC010111, in press.

Gill, A. E., J. S. A. Green, and A. J. Simmons, 1974: Energy partition in the large-scale ocean circulation and the production of mid-ocean eddies. *Deep-Sea Res. Oceanogr. Abstr.,* **21,** 499–528, doi:10.1016/0011-7471(74)90010-2.

Jenkins, W. J., D. J. McGillicuddy, and D. E. Lott, 2008: The distributions of, and relationship between, ^{3}He and nitrate in eddies. *Deep-Sea Res. II,* **55,** 1389–1397, doi:10.1016/j.dsr2.2008.02.006.

Large, W. G., and S. Pond, 1981: Open ocean momentum flux measurements in moderate to strong winds. *J. Phys. Oceanogr.,* **11,** 324–336, doi:10.1175/1520-0485(1981)011<0324:OOMFMI>2.0.CO;2.

——, J. C. McWilliams, and S. C. Doney, 1994: Oceanic vertical mixing: A review and a model with a nonlocal boundary layer

parameterization. *Rev. Geophys.,* **32,** 363–403, doi:10.1029/94RG01872.

Ledwell, J. R., A. J. Watson, and C. S. Law, 1993: Evidence for slow mixing across the pycnocline from an open-ocean tracer-release experiment. *Nature,* **364,** 701–703, doi:10.1038/364701a0.

——, ——, and ——, 1998: Mixing of a tracer released in the pycnocline. *J. Geophys. Res.,* **103,** 21 499–21 529, doi:10.1029/98JC01738.

——, D. J. McGillicuddy, and L. A. Anderson, 2008: Nutrient flux into an intense deep chlorophyll layer in a mode-water eddy. *Deep-Sea Res. II,* **55,** 1139–1160, doi:10.1016/j.dsr2.2008.02.005.

Li, Q. P., D. A. Hansell, D. J. McGillicuddy Jr., N. R. Bates, and R. J. Johnson, 2008: Tracer-based assessment of the origin and biogeochemical transformation of a cyclonic eddy in the Sargasso Sea. *J. Geophys. Res.,* **113,** C10006, doi:10.1029/2008JC004840.

Martin, A. P., and K. J. Richards, 2001: Mechanisms for vertical nutrient transport within a North Atlantic mesoscale eddy. *Deep-Sea Res. II,* **48,** 757–773, doi:10.1016/S0967-0645(00)00096-5.

McGillicuddy, D. J., and Coauthors, 2007: Eddy/wind interactions stimulate extraordinary mid-ocean plankton blooms. *Science,* **316,** 1021–1026, doi:10.1126/science.1136256.

McWilliams, J. C., and G. R. Flierl, 1976: Optimal, quasigeostrophic wave analyses of MODE array data. *Deep-Sea Res. Oceanogr. Abstr.,* **23,** 285–300, doi:10.1016/0011-7471(76)90871-8.

Schmitz, W. J., and P. L. Richardson, 1991: On the sources of the Florida Current. *Deep-Sea Res.,* **38,** S379–S409, doi:10.1016/S0198-0149(12)80018-5.

Smith, R. D., J. K. Dukowicz, and R. C. Malone, 1992: Parallel ocean circulation modeling. *Physica D,* **60,** 38–61, doi:10.1016/0167-2789(92)90225-C.

——, M. E. Maltrud, F. O. Bryan, and M. W. Hecht, 2000: Numerical simulation of the North Atlantic Ocean at 1/10°. *J. Phys. Oceanogr.,* **30,** 1532–1561, doi:10.1175/1520-0485(2000)030<1532:NSOTNA>2.0.CO;2.

Wunsch, C., 1997: The vertical partition of horizontal kinetic energy. *J. Phys. Oceanogr.,* **27,** 1770–1794, doi:10.1175/1520-0485(1997)027<1770:TVPOOH>2.0.CO;2.

Zhai, X., and R. J. Greatbatch, 2007: Wind work in a model of the northwest Atlantic Ocean. *Geophys. Res. Lett.,* **34,** L04606, doi:10.1029/2006GL028907.